Indian Journal of Pure & Applied Physics
Vol. 57, December 2019, pp. 923-927

Tuning of photonic bandgap in lithium niobate photonic crystal slab structures for wavelength filtering

Vadapalli Durga Rama Pavan* & Sourabh Roy
Department of Physics, National Institute of Technology, Warangal 506 004, India

Received 10 May 2019; accepted 3 October 2019

In this paper, photonic bandgap of Lithium Niobate ($LiNbO_3$) based photonic crystal slab with triangular lattice is presented and the tuning of bandgap is discussed as a function of slab's temperature. A micro-heater with plates parallel to the structure has been assumed for creating localized uniform heating and the corresponding refractive indices and dielectric constants were calculated using thermo-optic effect. MIT photonic bands software is used for the simulations. Tuning of band gap is performed at two wavelengths 632 nm and 1550 nm. It has been observed that the band gap is changing with temperature. The proposed structures can have the applications in wavelength filters, optical interconnectors and optical routers.

Keywords: Photonic bandgap tuning, Photonic bandgap structures, Wavelength filters, Thermo-optic effect

1 Introduction

Photonic crystals (PC) are gaining the attention of both scientific and commercial fraternities due to their extensive light controlling and modulating applications[1]. These are the structures formed by periodic arrangement of refractive index[2] (RI), for achieving specific applications like transmission or reflection of band of frequencies, the slowdown of light, parametric amplification, optical switching and non-linear effects[1,3-9]. The periodic arrangement of the RI is achieved by various methods, including creating air holes or cylindrical rods in a slab of semiconductor material, and arranging micro-spheres with different dielectric constants[2,10-11]. These structures exhibit photonic bandgap (PBG) which determines the frequency of operation. The band gap of a PC depends on the geometry of the structure and the RI of the material from which it is fabricated[12-15]. Most common method of tuning the band gap and dispersion features of a PC is tailoring its geometry[16-18]. Therefore, once the PC is fabricated, one cannot alter its PBG or the frequency of operation.

Tuning of the PBG and modes are becoming popular in the recent years for achieving specific applications. Careful designing of a line-defect based PC with various geometrical widths provides tiny but strong tunability[18]. PBG can be tunable in semiconductor based PC if the free-carrier density is high[19]. In this method, temperature of the slab and impurity concentration plays an important role[19]. Infiltration of liquid crystals into the silicon matrix provides the tunable PBG structures for the interconnectors[20,21]. Insertion of $KTaO_3$ crystal in the PC lattice provides the high tunability due to strong temperature[22] dependence of the $KTaO_3$. Electric field based tuning of the PBG is presented in GaAs based PC[7] and in a one-dimensional PC consisting of two Bragg mirrors[23]. These structures are finding precise and interesting applications like wavelength filters, optical interconnectors, dispersion compensation, and optical routers.

In the present work, tuning of PBG is presented for wavelength filtering applications. The RI of the slab material is considered as varying by adopting thermo-optic effect[24]. This can be realized by creating localized heating of PC by a micro-heater. Here, Lithium Niobate ($LiNbO_3$) based PC with air holes, arranged in a triangular lattice are considered as the base structure[25]. Initially, the bandgap of the structure is calculated at room temperature. Later, by implementing thermo-optic effect[24, 26-29], the RI of the slab and its dielectric constant values are calculated at two wavelengths 632 nm and 1550 nm at temperatures ranging from 20 °C to 75 °C. Here, 632 nm is chosen because of the extensive availability of He-Ne laser source and 1550 nm is selected because of its importance in the optical fiber communication.

*Corresponding author (E-mail: pavan4physics@gmail.com)

However, the designs can be extended to any wavelength depending on the geometrical parameters such as lattice constant of the structure and radius of the holes. These calculated dielectric constant values are used during the simulation, performed in open source software MIT photonic bands (MPB)[30]. The results reveal that the band gap is increasing with temperature.

2 Schematic of the Device

A triangular lattice based PC with air holes is used as the basic slab structure[25]. Air holes with radius of 0.3 times of lattice constant were assumed in the $LiNbO_3$ slab for creating the structure. This slab can be used directly in on-chip fabrication of photonic circuits or can be connected with a polymer fiber to fix in the optical network. A set of parallel plates, on both the sides of the PC is assumed to create localized heating and to act as a micro-heater. These plates are connected to an electric driving circuit for controlling the temperature of the slab. The schematic of the proposed device is shown in the Fig. 1.

The driving circuit keeps the slab at desired temperature and alters the RI of the slab via thermo-optic effect, leading to the tuning of band gap. These variations are useful for wavelength selection and filtering.

3 Theory and Methods

3.1 Modes in the PC

In order to calculate the eigen frequencies of the structure, one needs to consider the Maxwell's equations with suitable boundary conditions. The modes of the crystal can be solved by utilizing plane wave expansion method. The modes in the triangular lattice are indexed by k_z, $k_{\|}$ and *n*. These directions of the modes are shown in the Fig. 2.

The air columns are having a radius *'r'* and are separated with lattice constant *'a'*. The dielectric constant of the columns is 1. The periodicity exists in *x*, and *y* directions. On the other side, the refractive index is constant in the *z* direction. To adopt the Bloch's theorem, a periodic function $\vec{u}(\vec{\rho})$ must be defined and is considered as $\vec{u}(\vec{\rho})=\vec{u}(\vec{\rho}+\vec{R})$ for all lattice vectors $\vec{R}$. The existing Bloch states[1] in the structure can be written as:

$$\vec{H}_{(n,k_z,\vec{k}_{\|})}(\vec{r})=\exp\left[i\vec{k}_{\|}\cdot\rho\right]\exp\left[ik_z z\right]\vec{u}_{(n,k_z,\vec{k}_{\|})}(\vec{\rho})$$

where, $\vec{\rho}$ is the projection of *'r'* in the *xy*-plane; $n, k_z, \vec{k}_{\|}$ are the modes existing in the crystal. This equation after solving, results with the eigen states existing in the structure. In the present case, MPB is used on the Ubuntu platform for performing the simulations to obtain the eigen states of the structure.

3.2 Tuning of RI

Thermo-optic effect suggests that the RI of a material varies as a function of temperature[24]. According to Hobden and Warner[26], the RI of the O-ray of pure $LiNbO_3$ at visible and near infrared regions is given by:

$$n_o^2=4.9130+\frac{1.173\times10^5+1.65\times10^{-2}T^2}{\lambda^2-\left(2.12\times10^2+2.7\times10^{-5}T^2\right)^2}-2.78\times10^{-8}\lambda^2$$

and for the E-ray

$$n_e^2=4.5567+2.605\times10^{-7}T^2+\frac{0.970\times10^5+2.70\times10^{-2}T^2}{\lambda^2-\left(2.01\times10^2+5.4\times10^{-5}T^2\right)^2}-2.24\times10^{-8}\lambda^2$$

where, *T* corresponds to the temperature of the sample and λ corresponds to the operating wavelength. The refractive index of the material is calculated at the temperature range 20 °C to 75 °C and at two wavelengths 632 nm and 1550 nm. From these RI values, corresponding dielectric constants are calculated. These values are used in the simulation for calculating the eigen frequencies and band structure of the PC. From the obtained output, band structure and the PBG are calculated. The data is used for further analysis.

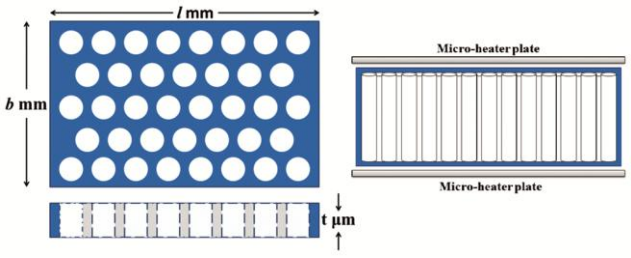

Fig. 1 – Schematic of the proposed device.

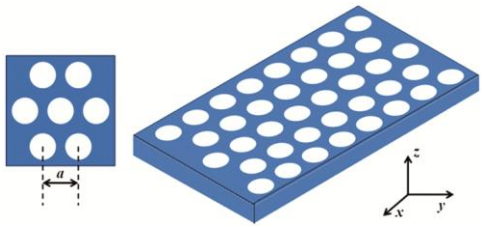

Fig. 2 – Triangular lattice formed by air columns in $LiNbO_3$ slab.

4 Results and Discussion

Initially the structure's frequency bands are calculated using the MPB software. These frequencies are plotted against the 'k' vectors of the structure. From the band structures, the PBG of the proposed structure with $LiNbO_3$ slab is calculated at two different wavelengths 632 nm and 1550 nm. The obtained band diagrams are shown in the Fig. 3.

From the band structure, it is clear that the PBG exists between band 7 and band 8. As these graphs are plotted against the normalized frequency, the lattice constant must be introduced to find the frequency of operation. Here, finding the position of band 7 and band 8 is sufficient enough to calculate the PBG and its shift with temperature. To tune the PBG with temperature, thermo-optic effect is introduced in the simulation process by adopting Eq. 1. For this, the calculated dielectric constants at 632 nm and 1550 nm at temperature range 20 °C to 75 °C are used in the input of the program and the corresponding frequency bands are calculated. From this data position of band 7, band 8 and the bandgap of the PC at every temperature interval is calculated. These are discussed in the subsequent sections.

The simulated results are analysed for understanding the band shift and tuning of PBG with temperature. For this, the positions of band 7 and band 8 at the wavelength range of 632 nm and 1550 nm are plotted against the temperature and are shown in the Fig. 4.

From the plots, one can conclude that the bands are shifting with temperature. As the increase in temperature introduces thermal expansion in the system, the effect of expansion is included in the simulation process, using the coefficient of thermal expansion of $LiNbO_3$ which takes the values $1.44\times10^{-5}\,K^{-1}$ for X-cut crystal, and $1.59\times10^{-5}\,K^{-1}$ for Y-cut crystal[31]. The increase in the radius of air holes

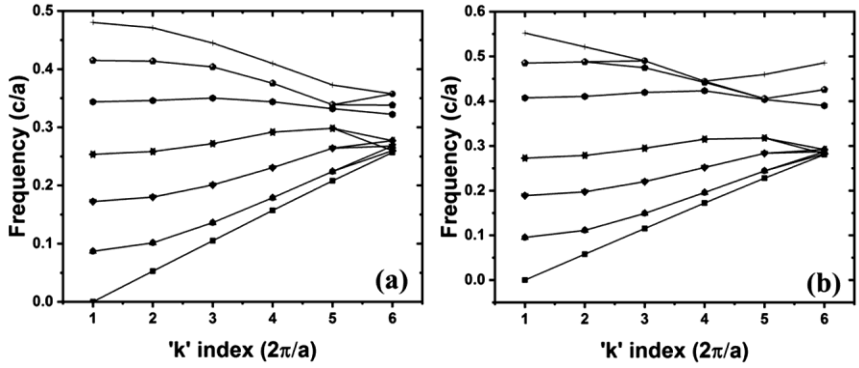

Fig. 3 – Band diagrams of the proposed structure (a) TM-modes at 632 nm and (b) TE-modes at 1550 nm.

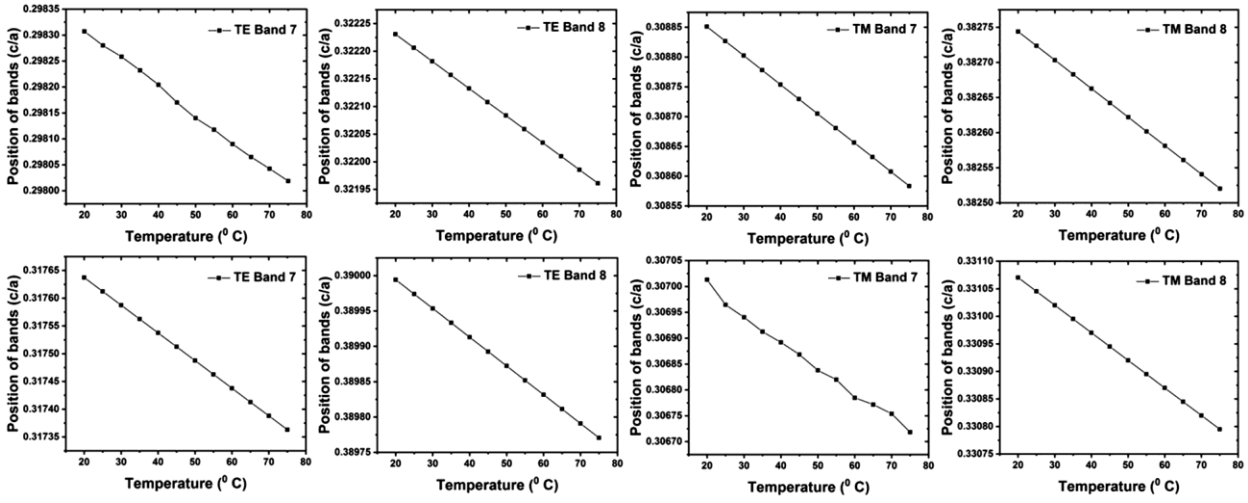

Fig. 4 – Change in position of bands with temperature. First row represents the TE and TM bands shift at 632 nm and second row represents the TE and TM bands shift at 1550 nm.

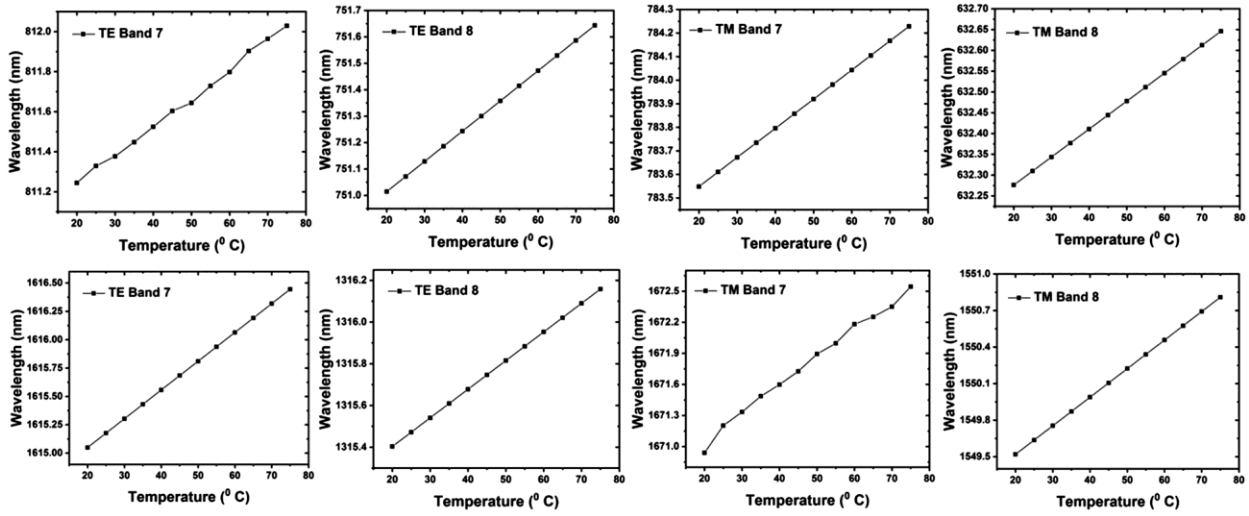

Fig. 5 – Shift in the eigen wavelength of PC with temperature. First row represents the TE and TM modes at 632 nm and second row represents the TE and TM modes at 1550 nm.

and lattice constant with temperature are calculated and used in the input of the program. However, the bands are not shifting due to the minute changes in the lattice constant of the PC and the radius of holes.

The eigen frequency purely depends on the lattice constant of the geometry of the PC. Hence, for achieving the wavelength filters in the range of 632 nm and 1550 nm the lattice constants are needs to be evaluated. Here the lattice constants are chosen in such a way that the eigen wavelength exists around band 8 of TM mode and shifts with temperature. These values are found to be 242 nm and 513 nm for eigen wavelengths of 632 nm and 1550 nm, respectively. With the implication of these lattice constants, corresponding eigen wavelengths are calculated and are plotted against the temperature of the slab and are shown in the Fig. 5.

The plots clearly states that the eigen wavelength and the PBG are shifting with the temperature. Keeping the wavelength of operation at the edge of the band gap provides efficient wavelength filters. Here the eigen wavelength is places around band 8 in both the cases for filtering applications. However the quick heating and cooling of the device makes this device more efficient and suitable for all optical applications.

5 Conclusions

A theoretical model for the tuning of the PBG of a PC slab through thermo-optic effect is proposed and the variations in the band gap are studied. It is found that the bands of the proposed system are shifting with temperature. The variations are expected to be still higher at higher values of temperature. The proposed system can have on-chip applications for switching of signals, all optical devices and switching applications in communication networks. It can be used as a wavelength filter and wavelength selector in optical sources.

Acknowledgement

Authors sincerely thank Department of Science and Technology, Government of India for funding this work through INSPIRE fellowship (IF160435).

References

1 Joannopoulos J D, Johnson S G, Winn J N & Meade R D, *Photonic Crystals: Molding the Flow of Light*, 2nd Edn, (Princeton University Press: New Jersey), 2008.

2 Joannopoulos J D, Villeneuve P R & Fan S, *Solid State Commun*, 102 (1997) 165.

3 Vlasov Y A, O'Boyle M, Hamann H F & McNab S J, *Nature*, 438 (2005) 65.

4 Baba T, *Nat Photonics*, 2 (2008) 465.

5 Roy S, Santagiustina M, Colman P, Combrie S & Rossi A D, *IEEE Photonics J*, 4 (2012) 224.

6 Coen S, Chau A, Leonhardt R, Harvey J D, Knight J C, Wadsworth W J & Russell P J, *J Opt Soc Am B*, 19 (2002) 753.

7 Pavan V D R, Roy S & Shankar M S, *Electrically Tuned Bandgap Structures for Optical Switching Applications*, 18p-221B-15, (JSAP-OSA Joint Symposia: Nagoya) 2018.

8 Monat C, Ebnali-Heidari M, Grillet C, Corcoran B, Eggleton B J, White T P, Faolain L O, Li J & Krauss T F, *Opt Express*, 18 (2010) 22915.

9 Monat C, Corcoran B, Pudo D, Ebnali-Heidari M, Grillet C, Pelusi M D, Moss D J, Eggleton B J, White T P, Faolain L O & Krauss T F, *IEEE J Quantum Electron*, 16 (2010) 344.

10 Fei Z, Liang W, San-Shui X & Sai-Ling H, *Chinese Phys Lett*, 19 (2002) 73.
11 Vlasov Y A, Bo X Z, Sturm J C & Norris D J, *Nature*, 414 (2001) 289.
12 Chutinan A, Imada M & Noda S, *Nature*, 407 (2000) 608.
13 Yablonovitch E, *J Mod Opt*, 41 (1994) 173.
14 Imagawa S, Edagawa K, Morita K, Niino T, Kagawa Y & Notomi M, *Phys Rev B - Condens Matter Mater Phys*, 82 (2010) 115116.
15 Soukoulis C M, *Photonic Band Gaps and Localization*, (Springer: USA), 2013.
16 Poli F, Cucinotta A, Selleri S & Bouk A H, *IEEE Photonics Technol Lett*, 16 (2004) 1065.
17 Frandsen L H, Lavrinenko A V, Fage-Pedersen J & Borel P I, *Opt Express*, 14 (2006) 9444.
18 Notomi M, Shinya A, Yamada K, Takahashi J, Takahashi C & Yokohama I, *IEEE J Quantum Electron*, 38 (2002) 736.
19 Halevi P & Ramos-Mendieta F, *Phys Rev Lett*, 85 (2000) 1875.
20 Weiss S M, Haurylau M & Fauchet P M, *Opt Mater*, 27 (2005) 740.
21 Pustai D M, Sharkawy A, Shi S & Prather D W, *Appl Opt*, 41 (2007) 5574.
22 Nemec H, Duvillaret L, Garet F, Kuzel P, Xavier P, Richard J & Rauly D, *J Appl Phys*, 96 (2004) 4072.
23 Skoromets V, Nemec H, Kadlec C, Fattakhova-Rohlfing D & Kuzel P, *Appl Phys Lett*, 102 (2013) 241106.
24 Saleh B E A & Teich M C, *Fundamentals of Photonics*, 2nd Edn, (Wiley: New York), 2007.
25 Takayama S I, Kitagawa H, Tanaka Y, Asano T & Noda S, *Appl Phys Lett*, 87 (2005) 2003.
26 Hobden M V & Warner J, *Phys Lett*, 22 (1966) 243.
27 Schlarb U & Betzler K, *Phys Rev B*, 48 (1993) 15613.
28 Smith D S, Riccius H D & Edwin R P, *Opt Commun*, 17 (1976) 332.
29 Boyd G D, Bond W L & Carter H L, *J Appl Phys*, 38 (1967) 1941.
30 MIT Photonic Bands: http://ab-initio.mit.edu/mpb/doc/mpb.pdf
31 Kim Y S & Smith R T, *J Appl Phys*, 40 (1969) 4637.